Analysis of Multipactor Effects by a Particle-in-Cell Algorithm Coupled with the Furman-Pivi Secondary Electron Emission Model

Dong-Yeop Na, Julio L. Nicolini and Fernando L. Teixeira
ElectroScience Laboratory, The Ohio State University
Columbus, OH 43212 USA
email: {na.94, nicolini.5, teixeira.5}@osu.edu

***Abstract*—We investigate multipactor effects due to secondary electron emission (SEE) using an electromagnetic particle-in-cell (EM-PIC) algorithm implemented on unstructured grids with the Furman-Pivi probabilistic SEE model. The present EM-PIC algorithm yields an energy- and charge-conserving time-update for fields and particles on unstructured grids, from first principles. The Furman-Pivi model enables a realistic description of SEE in EM-PIC simulations. We study the effects of the surface roughness for the reduction of secondary electron yield (SEY) on copper surfaces.**

I. Introduction

Multipactor is an effect associated with secondary electron emissions (SEE) at conducting or dielectric surfaces arising in resonance with an external RF field and leading to exponential electron multiplication [1]. Multipactor can affect many applications related to high power microwaves (HPM) [2]. In particular, multipactor is of great concern for satellite payloads due to the harsh space weather conditions conducive to SEE. On the other hand, multipactor can be harnessed in applications such as electron guns, plasma displays, and so forth [3]. For several decades, multipactor has been studied based on approximate analytical approaches and experimental data; however, with the dramatic rise of computational speeds in recent years, accurate numerical analysis has become feasible to bridge the gap between analytic and experimental works, particularly through electromagnetic particle-in-cell (EM-PIC) algorithms [4]. EM-PIC algorithms solve Maxwell-Vlasov describing the interaction of a large number of charged particles (collisionless plasma) and the electromagnetic field [5].

In this summary paper, we discuss the numerical analysis of multipactor effects using an EM-PIC algorithm coupled with the Furman-Pivi probabilistic SEE model [6]. The present EM-PIC algorithm yields energy and charge conservation from first principles on unstructured grids [7]–[10]. The algorithm is constructed based on the exterior calculus framework [11]–[13] and the use of Whitney forms [12]–[14] to expand the electromagnetic field degrees of freedom on the grid. The use of unstructured grids enables the representation of complex geometries with minimal defeaturing. Our study investigates the effects of surface roughness as a strategy to mitigate multipactor. We also investigate the saturation process in the electron population arising from the mismatch between the external RF acceleration and the space-charge self-field.

II. Algorithm Description

Due to computational constraints, PIC algorithms are based on a coarse-graining of the phase space where a collection of charged particles is replaced by a smaller set of superparticles. In EM-PIC algorithms, the temporal dynamics of each superparticle is simulated by performing four serial operations at each time step: (1) field update, (2) gather, (3) particle pusher, and (4) scatter. These four operations are described in detail elsewhere [7]–[10]. In addition, for multipactor problems, it is necessary to implement a SEE model at surfaces. Here, we implement a Monte Carlo based Furman-Pivi probabilistic SEE model with three components in the secondaries: (1) back-scattered (almost elastic), (2) re-diffused (inelastic), and (3) true-secondary (almost inelastic). For every single primary impact, the present algorithm evaluates the total number, the launching kinetic energy, and the angle of the secondary electrons under certain physical and mathematical constraints [6].

III. Numerical examples

Consider two parallel metallic plates separated by a gap $D_{\text{pp}} = 0.002$ [m] and fed by a RF alternating current source. The resonant condition for multipactor is given by

$$f_{\text{RF}} = \frac{1}{2\sqrt{\pi}D_{\text{pp}}}\sqrt{V_{\text{RF}}^{a}\frac{q_e}{m_e}} \quad \text{[Hz]} \tag{1}$$

where $f_{\text{RF}} = 2$ [GHz] and $V_{\text{RF}} = 1,143.16$ [V] are the frequency and RF voltage amplitude of the input signal, and q_e and m_e are the electron charge and mass, respectively. The entire problem domain is discretized by a two-dimensional unstructured (irregular) grid. The left and right sides of the domain are truncated by perfectly matched layers (PML) [15] to mimic open side boundaries. The metallic surfaces are modeled as perfect electric conductors (PEC) for the purpose of implementing the field boundary conditions. We initially place $1,000$ superparticles uniformly distributed near the lower plate, and launch them with zero velocities. In the simulations, each superparticle represents 2×10^7 electrons. In order to avoid large lateral electron spreading, the actual metallic

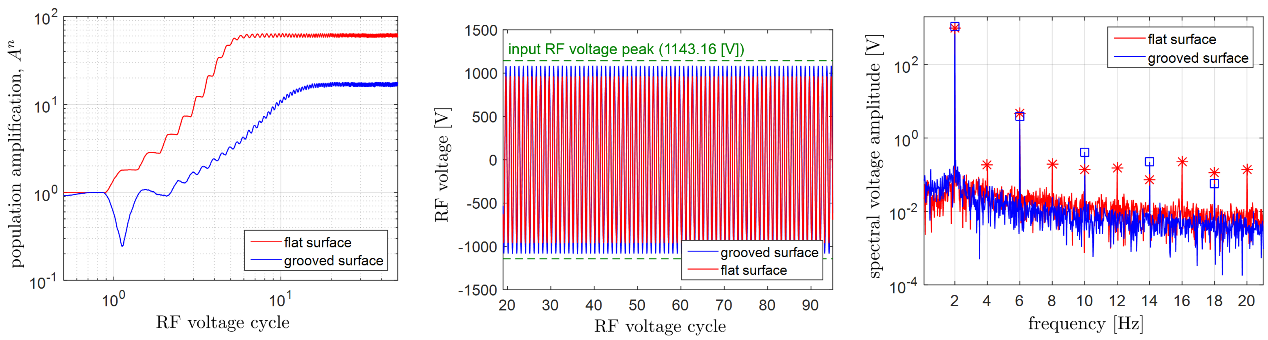

(a) (b) (c)

Fig. 1: Multipactor saturation effect. (a) Population amplification factor A^n versus RF voltage cycle. (b) Output signal in the time domain. (c) Output signal in the frequency domain.

plate yielding the secondaries covers a lateral extension of $L_{\text{mp}} = 0.03$ [m], while the other surfaces comprise collectors (i.e. absorbing electrons). Here we compare multipactor effects on flat and triangularly-grooved surfaces, and the role played by the groove angle. It has been suggested before that adequate choices for the latter can mitigate multipactor [16]. The width, depth, angle, and number of the grooves are given by $w_g = 0.0002$ [m], $h_g = 0.00055$ [m], $\alpha_g = 40^o$, and $N_g = 150$, respectively. We employ a local mesh refinement technique near the grooves to accurately model the near-singular field behavior near the tips. In order to capture the saturation process, we ran EM-PIC simulations for both types of surfaces up to 100 RF periods and measured the population change in stray electrons and the output signals. Fig. 1a illustrates the electron population amplification factor A^n versus RF voltage cycle, with $A^n = N_p^n / N_p^0$ where N_p is total number of superparticles flying between two metallic plates at the n^{th} time step of the simulation. Exponential electron multiplication is observed during the initial build-up. After several RF cycles, saturation occurs because strong space-charge self fields pulls back emitted electrons to the surface. On the other hand, in the intermediate stage, the amplitude of external RF fields prevails over the self field and most secondaries can escape from the emitted surface. It is interesting to observe that the electron population in the grooved surface is about half that of the flat surface case. In addition, the grooved surface case exhibits a smaller electron population in the saturation regime. Fig. 1b and Fig. 1c show output signals for both surfaces in the time and frequency domains, respectively. As expected, the output power loss due to multipactor in the flat surface case is more severe than in the grooved surface case as can be observed by a higher drop in the amplitude of the time domain signal in the former case. In addition, generally stronger harmonics of the fundamental frequency (2 [GHz]) are present in the flat surface case, as seen in the frequency domain plot.

Acknowledgment

This work was supported in part by NSF grant ECCS-1305838, DTRA grant HDTRA1-18-1-0050, and OSC under grants PAS-0061 and PAS-0110.

References

[1] J. R. M. Vaughan, "Multipactor," *IEEE Trans. Electron Devices*, vol. 35, no. 7, pp. 1172–1180, July 1988.

[2] R. F. Parodi, "Multipacting," in *Proceedings, CAS - CERN Accelerator School: RF for Accelerators, Ebeltoft, Denmark, 8 - 17 Jun 2010*, 2011.

[3] R. A. Kishek, Y. Y. Lau, L. K. Ang, A. Valfells, and R. M. Gilgenbach, "Multipactor discharge on metals and dielectrics: Historical review and recent theories," *Phys. Plasmas*, vol. 5, no. 5, pp. 2120–2126, 1998.

[4] J. W. You, H. G. Wang, J. F. Zhang, S. R. Tan, and T. J. Cui, "Accurate numerical method for multipactor analysis in microwave devices," *IEEE Trans. Electron Devices*, vol. 61, no. 5, pp. 1546–1552, May 2014.

[5] R. W. Hockney and J. W. Eastwood, *Computer Simulation Using Particles*. New York: CRC Press, 1988.

[6] M. A. Furman and M. T. F. Pivi, "Probabilistic model for the simulation of secondary electron emission," *Phys. Rev. ST Accel. Beams*, vol. 5, p. 124404, Dec 2002.

[7] H. Moon, F. L. Teixeira, and Y. A. Omelchenko, "Exact charge-conserving scattergather algorithm for particle-in-cell simulations on unstructured grids: A geometric perspective," *Comput. Phys. Commun.*, vol. 194, pp. 43–53, 2015.

[8] D.-Y. Na, H. Moon, Y. A. Omelchenko, and F. L. Teixeira, "Local, explicit, and charge-conserving electromagnetic particle-in-cell algorithm on unstructured grids," *IEEE Trans. Plasma Sci.*, vol. 44, pp. 1353–1362, 2016.

[9] D.-Y. Na, Y. A. Omelchenko, H. Moon, B.-H. V. Borges, and F. L. Teixeira, "Axisymmetric charge-conservative electromagnetic particle simulation algorithm on unstructured grids: Application to microwave vacuum electronic devices," *J. Comput. Phys.*, vol. 346, pp. 295 – 317, 2017.

[10] D.-Y. Na, H. Moon, Y. A. Omelchenko, and F. L. Teixeira, "Relativistic extension of a charge-conservative finite element solver for time-dependent maxwell-vlasov equations," *Phys. Plasmas*, vol. 25, no. 1, p. 013109, 2018.

[11] B. He and F. L. Teixeira, "Differential forms, Galerkin duality, and sparse inverse approximations in finite element solutions of Maxwell equations," *IEEE Trans. Antennas Propag.*, vol. 55, pp. 1359–1368, 2007.

[12] F. L. Teixeira and W. C. Chew, "Lattice electromagnetic theory from a topological viewpoint," *J. Math. Phys.*, vol. 40, pp. 169–187, 1999.

[13] F. L. Teixeira, "Lattice Maxwell's equations," *Prog. Electromagn. Res.*, vol. 148, pp. 113–128, 2014.

[14] A. Bossavit, "Whitney forms: A class of finite elements for three-dimensional computations in electromagnetism," *IEE Proc., Part A: Phys. Sci., Meas. Instrum., Manage. Educ.*, vol. 135, pp. 493–500, 1988.

[15] B. Donderici and F. L. Teixeira, "Mixed finite-element time-domain method for transient Maxwell equations in doubly dispersive media," *IEEE Trans. Microw. Theory Techn.*, vol. 56, pp. 113–120, 2008.

[16] M. Pivi, F. K. King, R. E. Kirby, T. O. Raubenheimer, G. Stupakov, and F. Le Pimpec, "Sharp reduction of the secondary electron emission yield from grooved surfaces," *J. Appl. Phys.*, vol. 104, no. 10, p. 104904, 2008.